Single cell lineage and regionalization of cell populations during Medaka neurulation

Yukihiro Hirose[1,2,*], Zoltan M. Varga[3], Hisato Kondoh[1,4,*] and Makoto Furutani-Seiki[1]

[1]Kondoh Differentiation Signaling Project (ERATO/SORST), Japan Science and Technology Corporation, 14 Yoshida-Kawaracho, Sakyouku, Kyoto 606-8305, Japan
[2]Graudate School of Sciences, Kyoto University, Sakyo-ku, Kyoto, 606-8502, Japan
[3]University Freiburg, Institute Biology 1 (Zoology), Department of Developmental Biology, Hauptstrasse 1, D-79104 Freiburg, Germany
[4]Graduate School of Frontier Biosciences, Osaka University, 1-3 Yamadaoka, Suita, Osaka 565-0871, Japan
*Authors for correspondence (e-mail: hirose@dsp.jst.go.jp and kondohh@fbs.osaka-u.ac.jp).

Summary

To study the movement of individual cells and development of cell grouping during neurogenesis, we labeled single cells in early Medaka gastrula at stage 13 [13 hours post-fertilization (hpf)] with a fluorescent vital dye, and analyzed cells and their descendants using time-lapse live recording up to stage 24 (44 hpf). At stage 13, all future neural cells were located in a dorsal 140° sector of the embryo, and migrated toward the vegetal pole; but during stage 15 to 16, they converged towards the midline. Cells that contributed to later neural subdivisions initially formed overlapping populations, but after stage 16+ they formed non-overlapping cell groups having characteristics of tissue 'compartments', preceding development of morphologically distinct neural subdivisions. In early retinal development, a single compartment for future retinal cells was formed superficial to telencephalic and diencephalic compartments, but it was split into left and right eye components at stage 17 in parallel with anterodorsal movement of the diencephalic compartment. At stage 16+, when these compartments were established, *Pax6* expression initiated, but only in the laterally located subpopulation of the retina precursor. These observations revise the current view of bilateral retinal development. Continuous live recording of labeled single precursor cells and computer graphics-assisted data analysis, which are presented for the first time in this study, provide excellent means with which to analyze essential cellular processes in organogenesis.

Supplemental data available online

Key words: Single cell labeling, Live recording, Computer graphics, Neural subdivisions, Compartments, Retina, *Pax6*

Introduction

A key question in early organogenesis is how the basic plan of the nervous system is established during and after gastrulation. From a very early stage in neural development, the nervous system is organized into morphologically discernible subdivisions arranged in anteroposterior order, which later have distinct functions: telencephalon, diencephalon, midbrain, hindbrain and spinal cord, as well as the peripheral nervous system derived from placodes and neural crest.

Precursor cells of the nervous system do not stay in fixed areas in the early embryo but undergo extensive intermingling, a process that begins even before the onset of gastrulation (Hatada and Stern, 1994; Kimmel et al., 1990). However, after boundaries of neural subdivisions become morphologically discernible, cells appear to be confined to the area of individual neural subdivisions (Fraser et al., 1990; Inoue et al., 2000). Evidence also indicates that regulation of cell movement (Myers et al., 2002) and interactions between groups of cells that form distinct neural subdivisions (Varga et al., 1999) is required for the establishment of functional central nervous system (CNS) subdivisions. Thus, the formation of cell groups that contribute to the same neural subdivision is an essential step in development of the organized CNS.

Behavior of cells in neurogenesis has been studied employing cell labeling or cell transplantation techniques in zebrafish and chicken embryos (Couly and Le Douarin, 1988; Fernandez-Garre et al., 2002; Hatada and Stern, 1994; Woo and Fraser, 1995; Woo and Fraser, 1998). These studies indicate progressive separation of precursors of neural subdivisions. However, in these early studies only the initial and terminal locations of cell populations were compared, and data on cell movement between those two time points was missing. Therefore, the information has stopped short of understanding how cell groups for individual CNS subdivisions are organized from individual cells.

We report analysis of movement of a number of randomly chosen blastoderm cells by fluorescent labeling and live recording of single cells. We used Medaka fish (*Oryzias latipes*) embryos for analysis, taking advantage of embryo transparency, the wealth of knowledge on their development, and, in particular, the recent massive screening of gene mutations that affect nervous system development (Wittbrodt et al., 2002). From a practical view point, the slower

development of Medaka embryo compared with zebrafish facilitates the characterization of the sequence of events with high temporal accuracy. Time-lapse and long time span recording of a number of the same individual labeled cells in developing embryos allows understanding of how cell groups are organized and segregated, and how they undergo morphogenesis in the nervous system.

The analysis indicates that the cells that contribute later to distinct neural subdivisions start as overlapping populations in early blastoderm; however, at stage 16+, they almost synchronously segregate into non-overlapping cell populations that have the characteristics of 'compartments', with cell migration across compartments being inhibited and cell divisions not yielding daughter cells fated to distinct compartments. This synchrony of compartmentalization of neural subdivisions is probably different from that in zebrafish, where neural subdivisions are established in sequence from anterior to posterior (Woo and Fraser, 1995). This analysis also indicates how 'convergence and extension' (Myers et al., 2002) of neural cells takes place in Medaka, with 'extension' occurring only in the hindbrain and spinal cord.

Precursors for future retina form a single neural compartment at stage 16+ that overlays telencephalon and diencephalon. This retinal compartment was bisected into bilateral retina precursors in parallel with anterodorsal movement of the diencephalic precursor compartment, a movement that was previously indicated by single cell analysis in zebrafish embryos (Varga et al., 1999). As an extension of the analysis, we compared establishment of the retinal precursor compartment and expression of *Pax6*, observing a temporal lag between these events, and found that *Pax6* expression in the early phase was confined to laterally located cells in the retina-specified cell population.

Thus, dynamic, computer graphics-aided analysis of cell movement composed of continuous live recording of single labeled cells provides a powerful new tool for understanding cellular events in the embryo. The same technique should prove useful in non-neural tissues and in other animal species, but transparent fish embryos are especially advantageous, and Medaka allows high temporal resolution of events during gastrulation to be achieved.

Materials and methods

Fish and staging
Pigment-free 'see-through Medaka' (Wakamatsu et al., 2001) were used for all experiments. Embryos were obtained by natural spawning and incubated at 26°C in BSS+PS (Iwamatsu, 1994). Embryos were dechorionated using the hatching enzyme prepared according to Ishida (Ishida, 1944) (gift from Dr K. Niwa). Developmental stages of embryos were determined by the degree of epiboly progression, and according to the standard stage table (Iwamatsu, 1994) with additional definition of stages 15+ (19 hpf), 15++ (20 hpf), 16+ (22 hpf), 16++ (23 hpf) to describe dynamic changes in embryo occurring at the cellular level (Table 1, see Figs S1, S2 at http://dev.biologists.org/supplemental/).

Generation of 3D computer graphics assisted embryo models
To collect basic structural data on Medaka development, five embryos with a diameter of 1000 μm±10 μm at stage 13 (13 hpf, 25% epiboly) were selected and dechorionated. Development was allowed in 1.5%

methyl cellulose, and live images were taken at regular intervals. Diameter of embryos, length of dorsal cell thickening along the meridian from animal to vegetal poles, and the percentage of epiboly were scored. Structural data for embryos are summarized in Fig. S1 at http://dev.biologists.org/supplemental/. A three-dimensional computer graphics model was generated using these data and computer graphics software CINEMA 4D (MAXON). The model embryo is basically spherical, but local constriction along the leading edge of the blastoderm is introduced from stage 15 to stage 16++ to mimic live embryos (see Fig. S2 at http://dev.biologists.org/supplemental/).

Fluorescent single cell labeling
At stage 13 when embryos were spherical, embryos of 1000 μm ±10 μm diameter were selected for best fit to the computer graphics embryo model. Single cells were injected at this stage with 3% rhodamine dextran dye (Molecular Probes D-3308) using the technique described by Varga et al. (Varga et al., 1999). The thickened cell layer forming the embryonic shield at the dorsal margin was used as a landmark to orient the blastoderm. Dechorionated embryos were placed on a graded silicone mount and the animal pole was oriented upwards. One to three cells some distance apart in an embryo were then injected with fluorescent dye.

Time-lapse recording of the labeled cells and data analysis using computer graphics model of the embryo
At intervals of 1-2 hours, fluorescent images of the embryos were photo-recorded from multiple angles. Cells labeled with fluorescent dye were observed by mounting an embryo on a 1×1 mm grid reticules in a silicon mount and photo-recording from two angles (from stage 13 to stage 16) or three angles (dorsal, lateral and frontal) (stage 16 and later) using a Zeiss Axio Skop2 FS microscope equipped with a Pixera Penguin 150CL camera. Cell positions were transferred to the computer graphics model embryo in the following way. The stage-matched model embryo was oriented at the same angle as the photo-image of the live embryo using morphological landmarks, e.g. blastoderm edge and cell thickening along the dorsal midline. Images of real and model embryos were superimposed, and the position of a fluorescent cell observed from an angle was plotted onto the model. The plot was also made from the second angle, and the gravity center of the plots was taken as the cell position on the computer graphics model embryo. A cell is presented by a dot with a diameter of 20 μm that approximates cell diameter in real space (Fig. 1). Trajectories of labeled cells were generated using recorded positions and the Bezier spline curve approximation method in CINEMA 4D software (see Movie at http://dev.biologists.org/supplemental/).

In situ hybridization
Whole-mount in situ hybridization for *Pax6* was performed as described (Loosli et al., 1998), using BM purple (Boehringer) for color development of hybridization signals.

Results

Time-lapse live recording of fluorescence-labeled cells in a developing embryo
To understand how precursor cells move in the forming neural plate, and how they segregate and finally contribute to distinct neural subdivisions, we labeled single precursor cells with fluorescent vital dye rhodamine dextran, recorded positions of the cells and daughter cells in real time and transferred cell positions into a computer graphics animated embryo. Progression of embryogenesis was staged by introduction of new stages into the conventional table (Ishida, 1944) for more accurate description of events during gastrulation (Table 1).

Table 1. Developmental stages of Medaka embryo and major cellular events

Stage	Age (hpf)	% epiboly	Landmark events in morphological development	Major events in cell populations characterized in this study
13	13	25	Initiation of gastrulation	Neural precursors occupy the dorsal 140° sector region, and cells later contributing to anterior and posterior CNS occupy different territories
14	15	40		
15	17.5	50	Ingression of hypoblast under epiblast becomes visible	Neural precursor cells begin to converge towards the midline, resulting in segregation of neural/non-neural cells
15+	19	60		
15++	20	70		Last split fate cell division observed
16	21	80	Initiation of neural keel development	
16+	22	90		Establishment of 'compartments' by cell groups for different neural subdivisions. Initiation of animal pole directed movement of the compartments for anterior CNS
16++	23	95		
17	25	97	Thickening of brain-forming region	Initiation of bifurcation of the compartment of retinal precursors
18	26	98		
19	27.5	100 (2 somites)	Initiation of somitogenesis	Cell movement within compartments ceases
20	31.5	100 (4 somites)	Initiation of retina invagination	
21	35	100 (6 somites)	Appearance of otic vesicle	
22	38	100 (9 somites)	Appearance of heart primordium underneath the brain	
23	41	100 (12 somites)	Appearance of brain cavities	
24	44	100 (16 somites)	Development of morphologically distinct neural subdivisions; initiation of heart beat	

The images of a real embryo and stage-matched computer graphics model were superimposed and the positions of fluorescence-labeled cells in the embryo were plotted on the model (Fig. 1A,B). We plotted cells by using images at different angles of the same embryo, and the middle points of cell plots were taken for cell positioning. In practice, cell positions in the computer graphics embryo model were very accurate, and following plots could be merged with previous ones without exception (Fig. 1). After stage 16, cell positions in an embryo were measured from three directions (dorsal, lateral and frontal), as the embryos gained thickness along the midline. The standard deviation of cell position measurements at stage 15 was 7.0 µm (*n*=50), and that at stage 17 was 3.0 µm (*n*=50), while the average cell diameter was 20 µm.

Neural progenitors of the blastoderm

At stage 13 (13 hpf), early in gastrulation, the animal quarter of the yolk surface is covered by two-layered blastoderm. The outer layer consists of flat cells, while the inner layer is composed of round cells and has variable thickness from one to two cell diameters (ventral margin) to four to five cell diameters (dorsal margin). We determined the cell population that gave rise to neural tissue in later development by single cell labeling. Of 120 randomly labeled single cells at stage 13, 13 were in the outer layer, and descendants of all these cells were found in the enveloping layer at stage 24 (44 hpf, 16 somites). Early separation of blastoderm cells into these germ layers is common to fish species (Ballard, 1973; Kimmel et al., 1990; Oppenheimer, 1936; Warga and Nusslein-Volhard, 1999).

Among the remaining 107 cells in the inner layer that developed into embryonic tissues at stage 24, 75 initially located in the dorsal 140° sector (±70° latitude), referred to as the 'neurogenic sector' (Fig. 2C), contributed mainly to the neural and placodal tissues. Six cells of the same sector that were close to the blastoderm margin contributed to somitic mesoderm, and 26 cells outside of the dorsal sector contributed primarily to epidermis (Fig. 2C).

To study dynamics of cells initially located in the neurogenic sector of the blastoderm in neural development, we labeled 150 single precursor cells in the sector and surrounding regions in stage 13 (13 hpf) embryos and recorded their positions in developing embryos at 1-2 hour intervals for 31 hours, up to stage 24 (44 hpf). During the period, the labeled cells multiplied to 460 (roughly a threefold increase). Because the data indicated bilateral symmetry, data from the left and right halves of the embryo were mirror-imaged and superimposed. In zebrafish, development through corresponding stages proceeds in ~10 hours (Kimmel et al., 1995).

Initial cell populations that contribute later to the neural subdivisions

The nervous system of stage 24 embryo is subdivided common to vertebrates: telencephalon, retina, diencephalon, mesencephalon, rhombencephalon, spinal cord and peripheral nervous system of placodal or neural crest origin (Fig. 3C). The fluorescent-labeled cells at stage 13 were color-coded in the computer-graphics model according to their contribution to neural subdivisions at stage 24 (Fig. 3A,C-E)

At stage 13, cells that later contribute to the same neural subdivisions were not distributed randomly in the neural sector, but formed loose cell clusters occupying crescent-shaped territories and were arranged to reflect the AP order of future neural subdivisions. Territories of the future telencephalon (red), retina (green), diencephalon (black) and mesencephalon (orange) occupied almost the same embryonic region, while those for future rhombencephalon (blue) and spinal cord (white) were positioned more posteriorly and with an extensive regional overlap between the two (Fig. 3B). Therefore, there are two major domains in the neural sector, those contributing to the brain region anterior to the midbrain (green, red, black and orange) and those posterior to the hindbrain (blue and white).

Separation of epidermal and neural precursors (stage 13 to stage 16)

Along with progress of epiboly, initial movement of cells was largely vertical, as indicated by their trajectories at the beginning of gastrulation (Fig. 4). However, from stage 15 to stage 16, in contrast to epidermal cells that continued vertical
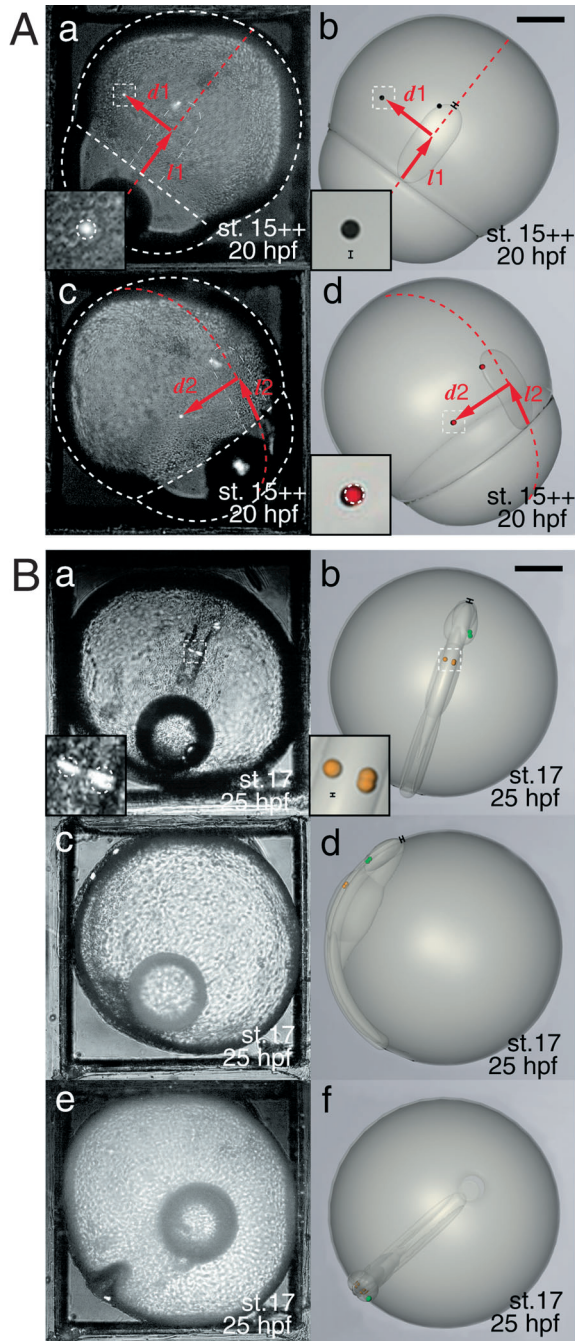
Fig. 1. Cell positions in live Medaka embryos and their transfer to a computer graphics model. (A) Two labeled cells in an embryo at stage 15++ (20 hpf). (a,c) Fluorescence images of the same embryo viewed from different angles. Broken white lines indicate outline of embryo, blastoderm edge and cell thickening along the dorsal midline. Images in a,c were superimposed on stage- and size-matched computer graphics models in b,d, and positions of the two fluorescent cells were plotted on the model using red and black dots, respectively. The diameter of dots corresponds to 20 μm, approximating average cell size. Insets in a,b,d are enlargements of the squares indicated by broken lines. The cell coordinates $l1$ (along the dorsal midline shown by red broken line) and $d1$ (distance along the circumference from the midline) of the first measurement (b) agreed with those of the second ($l2$ and $d2$), and two plots overlapped well (d). (B) Three cells at stage 17 (25 hpf). (a,c,e) Fluorescence images of dorsal, lateral and frontal angles. (b,d,f) Cell positions in a,c,e are plotted on the computer graphics model. Insets in a,b are enlargements of the small squares. The cells indicated by the green dots later contributed to retina, while those indicted by orange dots contributed to mesencephalon. Error bars indicate standard deviations in embryo length along the dorsal midline and positions of the plotted cells (insets). Scale bars: 200 μm.

stage 15 to stage 16, the areas of AP overlap of neighboring cell groups to follow different fates became smaller (Fig. 3G,H). Then, cell groups that contributed to different divisions of the CNS became clearly separated without future cell mixing after stage 16+ (22 hpf, 90% epiboly) (Fig. 3I,I′).

Immediately after stage 16+ (22 hpf), vertical movement of future neural cells became largely arrested, then the cells for telencephalon, retina, diencephalon and mesencephalon turned their directions towards the animal pole (Fig. 4B-E), while the cells for future rhombencephalon and spinal cord showed horizontal drift toward the midline (Fig. 4F,G).

As indicated by the rectangles in Fig. 3G-K and more explicitly by the illustrations of cell group positions in Fig. 5A, after stage 16+ cell groups for future tel-, di- and mesencephalon did not change their AP width significantly (telencephalon actually becomes shorter in the AP dimension), and were displaced anteriorly on the embryo coordinate as coherent cell masses. By contrast, the cell group for rhombencephalon became twice as long along the AP axis during the period from stage 16+ to stage 19. The area occupied by the prospective spinal cord cells was more posteriorly shifted and significantly elongated (Fig. 5A).

These movements of cells as cell groups are clearly reflected by the trajectories of individual cells after stage 16+ (Fig. 4). Trajectories of cells for tel-, di- and mesencephalon, and retina indicate massive anterior movement (Fig. 4B-E), while those for spinal cord showed only posterior movement (Fig. 4G).

Establishment of compartments for future neural subdivisions (stage 16+)

Spatial coherency of cells belonging to a future subdivision of the CNS after stage 16+ suggests that neural subdivisions are already established by this stage, much earlier than neural subdivisions became morphologically discernible (stage 24, 44 hpf). However, trajectories of individual cells (Fig. 4) indicate that cells change their relative positions after stage 16+. These observations suggest that cells do not cross the boundaries of neural subdivision once established at stage 16+, while cells change their relative positions within neural subdivisions, i.e.
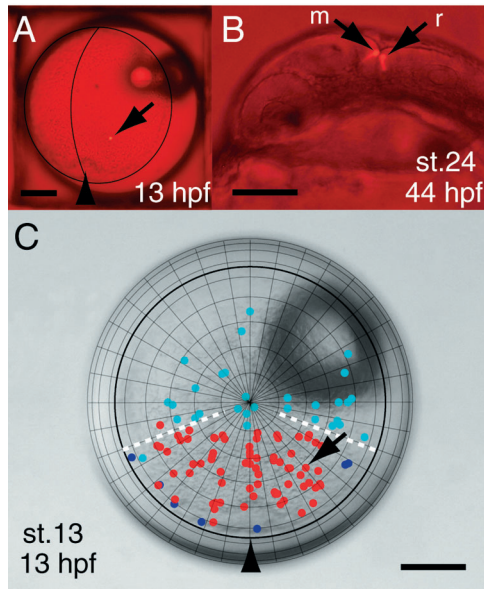
movement toward the vegetal pole, those contributing to neural subdivisions changed directions and converged near the midline (Fig. 4A). This difference of cell movements distinguishes and promotes separation of cell populations that later contribute to epidermis and neural tissues (Fig. 4A). Non-overlapping cell groups of epidermal and neural populations were established by stage 16, bordered by the cell population of future neural crest/placode (yellow) (Fig. 3H).

Separation of precursor cell populations for neural subdivisions (stage 16+).

During the period from stage 15 to stage 16+, cell populations for the individual neural subdivisions became separate. From

Fig. 2. Distribution in stage 13 blastoderm of cell populations that later gave rise to neural or non-neural tissues. (A) A single labeled precursor cell (arrow) at stage 13 embryo in animal pole view. The arrowhead indicates embryonic shield. (B) Anterior region of the same embryo at stage 24 (44 hpf) in lateral view. The single cell shown in A divided, and its daughter cells (arrows) were later fated to mesencephalon (m) and rhombencephalon (rhombomere 1) (r). (C) One hundred and seven randomly chosen cells of stage 13 (13 hpf) embryos, one to two cell diameters beneath the envelope layer, were labeled and their location in stage 24 embryos (44 hpf) was recorded. Labeled neural progenitor cells (including CNS, placodes and neural crest) are indicated by red dots and shown in animal pole view. Light blue dots represent cells that contributed to epidermis and purple dots to somitic mesoderm. The arrowhead indicates dorsal midline (embryonic shield). Blastoderm margin (leading edge of epiboly) is indicated by a circle. The dot with an arrow indicates the labeled cell shown in A. Broken lines highlight the 140° neurogenic sector. Scale bars: 200 μm.

between the boundaries. To confirm this, we assessed relative vertical migration of the cells at various AP levels from diencephalon to rhombencephalon during development from stage 15+ to 24, by counting the number of cells crossing horizontal lines transverse to the cell group (Fig. 5B, part a). During this period, all neural precursors of the corresponding subdivisions were displaced as a mass along the AP axis, without significant alteration of the AP length of individual territories. Lines 3 and 8 were placed on boundaries of the prospective di- and mesencephalon, and that of mes- and rhombencephalon, respectively (Fig. 5A). As shown in Fig. 5B (part b), up to stage 16, vertical movement in the cell population was almost uniform along the various AP levels, but at stage 16+, the movement across lines 3 and 8 was suddenly arrested, while at other AP levels vertical cell movement continued. This indicates that the cell groups that later form di, mes- and rhombencephalon organized separate 'compartments' where cells may move around in a compartment but do not cross boundaries with other compartments.

Vertical cell movement within the compartment remained extensive up to stage 17 (3 hours later), then after stage 19 the vertical cell movement across the lines were gradually attenuated. This temporal change in cell movement activity was also observed along the horizontal axis (Fig. 5B, part c). Measurement of lateral movement by counting cells crossing the midline (Fig. 5B, part c) indicated that this movement is maximum at stage 17, but is attenuated at stage 19.

Establishment of compartments at stage 16+ was supported by the observation on the fate of mitotic daughter cells (Fig. 5C). Some mitoses occurring in the region of cell group border gave rise to daughter cells with split fates up to stage 16, but after stage 16+ even those mitoses that took place very close to the border with another cell group never produced split fate daughters (Fig. 5C), although cell growth was more pronounced after this stage (Fig. 5D). Thus, establishment of a compartment results in clonal separation by the boundary.

Development of individual compartments for neural subdivisions

After cell groups are organized into compartments, there is a period of extensive cell proliferation around stage 17 (Fig. 5D), followed by a steady increase of cell number in all compartments. This cell proliferation was not accompanied by an increase in AP length of the anterior neural compartments (Fig. 5A), and resulted in a gain in their width and height (Fig. 3E,K, Fig. 5A). Thus, in Medaka embryos, overall 'convergence' of neural precursors towards the midline clearly occurs as illustrated by cell trajectories (Fig. 4), but 'extension' of the central nervous system is ascribed only to moderate AP elongation of the rhombencephalon and spinal cord.

Development and lateral separation of the single retinal population

We analyzed how two retinas are generated and separated into two eyes from a single, coherent cell group. Retina-forming cells were in a single compartment at stage 16+ (22 hpf) superficial to telencephalic and diencephalic compartments, and covering their posterior and anterior halves (Fig. 6A-C). This single retinal compartment was split bilaterally from posterior to anterior, paralleled with dorsal movement of diencephalic precursors (Fig. 6D-F). At the same time, the ventral region of the diencephalic cell group elongated anteriorly and displaced future telencephalic cells in the anterior and dorsal direction (Fig. 6C,F,I). By stage 19, the retinal cell group had been completely separated into two lateral groups (Fig. 6G-I). Thus, the bilateral retinas were established from an isolated single compartment by morphogenetic cell movement.

We compared morphogenetic events to form bilateral retinas and expression of *Pax6*. *Pax6* expression first became detectable at stage 16+ (22 hpf) only in laterally located populations of prospective retinal cells (Fig. 7A,B). Presumptive median retinal cells did not express *Pax6* although the retinal compartment was already established as a single field of cells, arguing against the view that Pax6 expression indicates establishment of retinal primordium.

Only 1 hour later (stage 16++, 23 hpf), as the retinal cell population was split and pushed aside, all presumptive retinal cells expressed *Pax6*. At the same time, *Pax6* was also expressed in all presumptive diencephalon precursor cells, and upregulated in rhombencephalon and spinal cord (Fig. 7C,D). These patterns of *Pax6* expression persisted to later developmental stages (Fig. 7E,F).

Fig. 3. Time course of cells labeled at stage 13 (13 hpf) and their descendants until stage 24 (44 hpf). (A) Precursor cell populations at stage 13 and (C-E) their descendants at stage 24. Throughout, cells are indicated by dots and color-coded according to the location of cell fates at stage 24 as indicated in (C): telencephalon (Tel, red); retina (Re, green); diencephalon (Di, black); mesencephalon (Mes, orange); rhombencephalon (Rho, blue); spinal cord (SC, white); epidermis (Epi, light blue); peripheral nervous system including placodes and neural crest (yellow); trunk mesoderm (pink). Data of left and right halves are superimposed assuming bilateral symmetry of the embryo. (A) Plots of cells on the embryo model at stage 13 in animal pole view (dorsal midline towards the bottom). Double-colored dots (e.g. arrowhead) in A indicate cells that contributed to two different neural subdivisions or tissues as shown by cells in Fig. 2A,B. A pair of cells located adjacent to one another at stage 13 are indicated by black and white arrows. These cells are indicated in the panels of later embryos, and at stage 24 (D,E) are located distantly in the diencephalon and rhombencephalon. (B) Outline of territories occupied by the groups of cells later

contributing to distinct neural subdivisions, which are indicated by the same color codes as the cells. (C) Neural subdivisions of Medaka at stage 24 illustrated with distinct colors. (D,E) Distribution of labeled cells in stage 24 embryo in side (D) and dorsal (E) views. (F-K) Distribution of color-coded cells on embryo model from stage 13 to stage 18. (F) Stage 13 (early gastrula, 13 hpf); (G) stage 15 (mid-gastrula, 17.5 hpf); (H) stage 16 (late gastrula, 21 hpf); (I) stage 16+ (late gastrula +, 22 hpf); (J) stage 17 (25 hpf); (K) stage 19 (two somites, 28 hpf). Cell groups forming individual neural subdivisions are clearly separated during the 1 hour period 21 hpf (stage 16) to 22 hpf (stage 16+). (A′,G′-K′) Enlargement of squares in A,G-K. Scale bars: 200 μm. Black and white arrows indicate two individual cells as in A-K
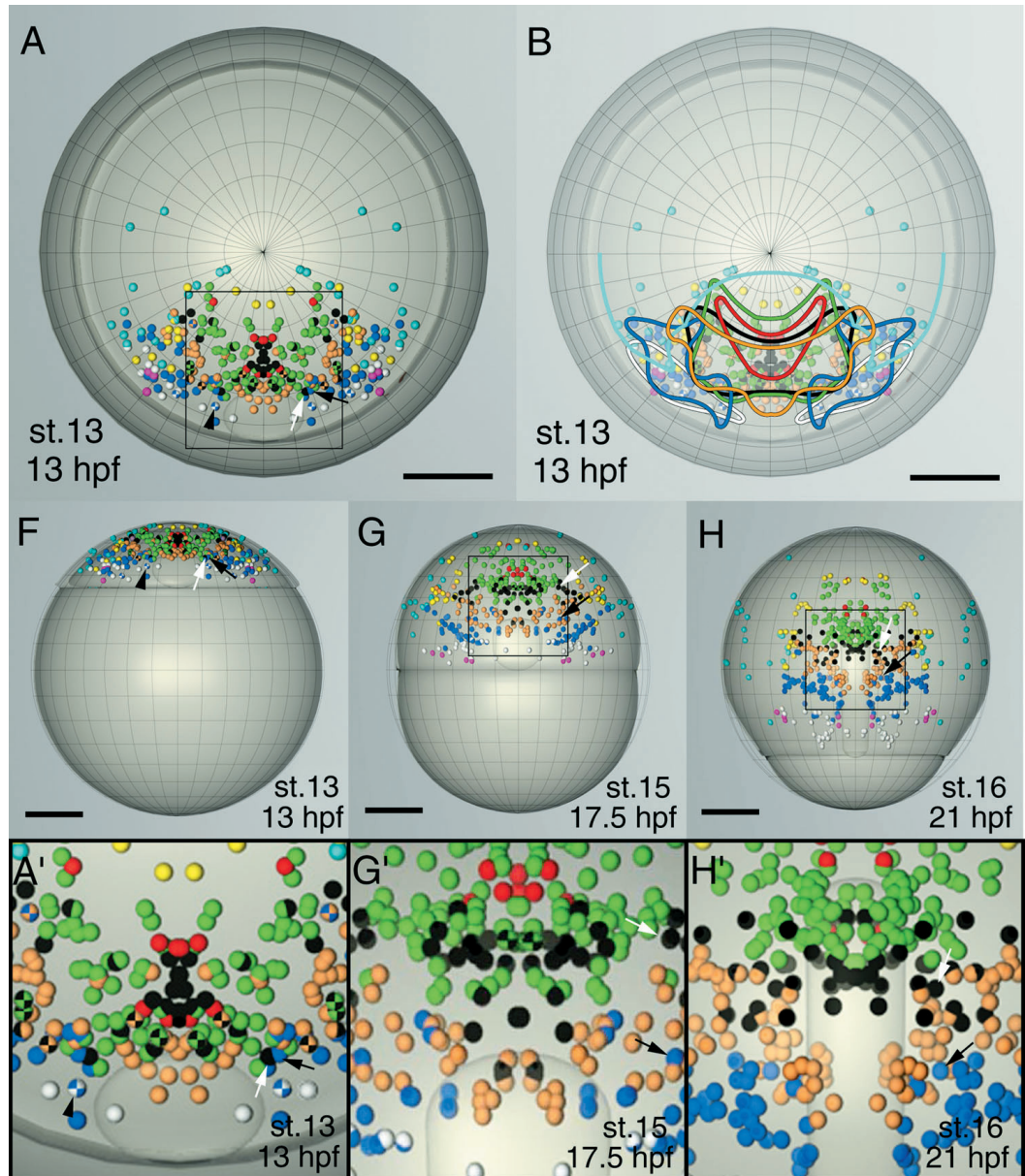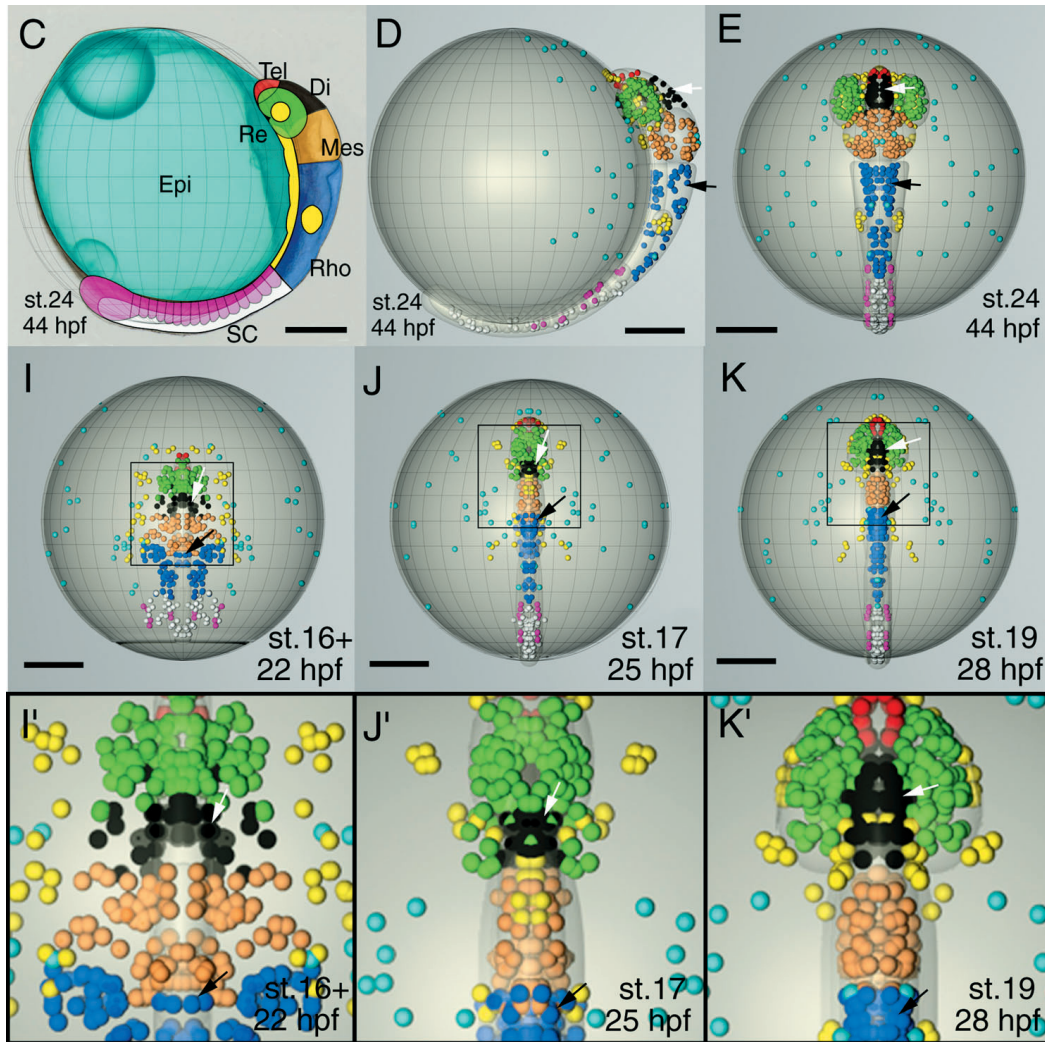
Discussion

Continuous positional recording of a number of randomly chosen, initially single labeled cells over the period of gastrulation and their analysis aided by computer graphics visualized how cell groups are organized to form future neural subdivisions and established as distinct 'compartments' of the CNS primordium (see Movie at http://dev.biologists.org/supplemental/). This was achieved for the first time in this work among vertebrates. Very high reproducibility in coordinates of embryonic subdomains on the spherical embryo surface (Fig. 1, see Fig. S1 at http://dev.biologists.org/ supplemental/) (Woo

and Fraser, 1995) and beautifully synchronous development among different embryos, a characteristic of fish species, provided the basis for successful analysis. Slower development of Medaka embryo compared with zebrafish allowed analysis of the sequence of events with a high temporal resolution.

Comparison with earlier analysis in particular on zebrafish

Pioneering studies traced cell fates in a large number of blastodermal cells using single cell labeling or analogous techniques in embryonic chicken and zebrafish (Fernandez-

C st.24 44 hpf; D st.24 44 hpf; E st.24 44 hpf; I st.16+ 22 hpf; J st.17 25 hpf; K st.19 28 hpf; I' st.16+ 22 hpf; J' st.17 25 hpf; K' st.19 28 hpf

forming different neural subdivisions is completely lost at all AP levels (Fig. 3).

(3) After stage 16+, cells that later form a neural subdivision organize a coherent cell cluster maintaining clear boundaries with other cell groups (Fig. 5A).

This synchrony of events among cell groups for future neural subdivisions is in a sharp contrast to zebrafish embryos (Woo and Fraser, 1995), where at 10 hpf separation of the cell groups for tel-, di- and mesencephalon is almost complete, but those of mes- and rhombencephalon still share a region of overlap, and rhombencephalic precursors have not converged to the midline.

Early characteristics of neural progenitor cells

In stage 13 embryos, all neural progenitor cells were located on the dorsal 140° sector of the deep cell layer (Fig. 2). Territories occupied by the progenitors of distinct neural subdivisions overlapped extensively (Fig. 3B). This observation argues that the later fate of precursor cells in stage 13 embryos is not strictly specified but depends on conditions such as cell position at a later developmental stage. Regional overlap of different cell fates in early blastoderm was also observed by labeling of cells in early zebrafish and chicken embryos (Hatada and Stern, 1994; Kimmel et al., 1990; Woo and Fraser, 1995).

Garre et al., 2002; Hatada and Stern, 1994; Woo and Fraser, 1995; Woo and Fraser, 1998). Specific attention was paid to genesis of the CNS, which occurs the earliest and occupies the largest cell population in the early embryos. These earlier works recorded positions of labeled cells at limited time points without following the behavior of cells in between. In this study, we performed time-lapse recording of single labeled cells over a relatively long time span (nearly 30 hours), enabling characterization of the sequence of events in great detail.

Work carried out by Woo and Fraser (Woo and Fraser, 1995) on zebrafish was particularly informative, and comparison of data on Medaka and zebrafish reveals common principal processes in early development in these fish species, but also highlights interesting differences. Thus, although neural subdivisions in zebrafish appear to be progressively formed anterior to posterior, in Medaka all neural subdivisions are formed and compartmentalized more or less synchronously. In Medaka there are three stages in the process.
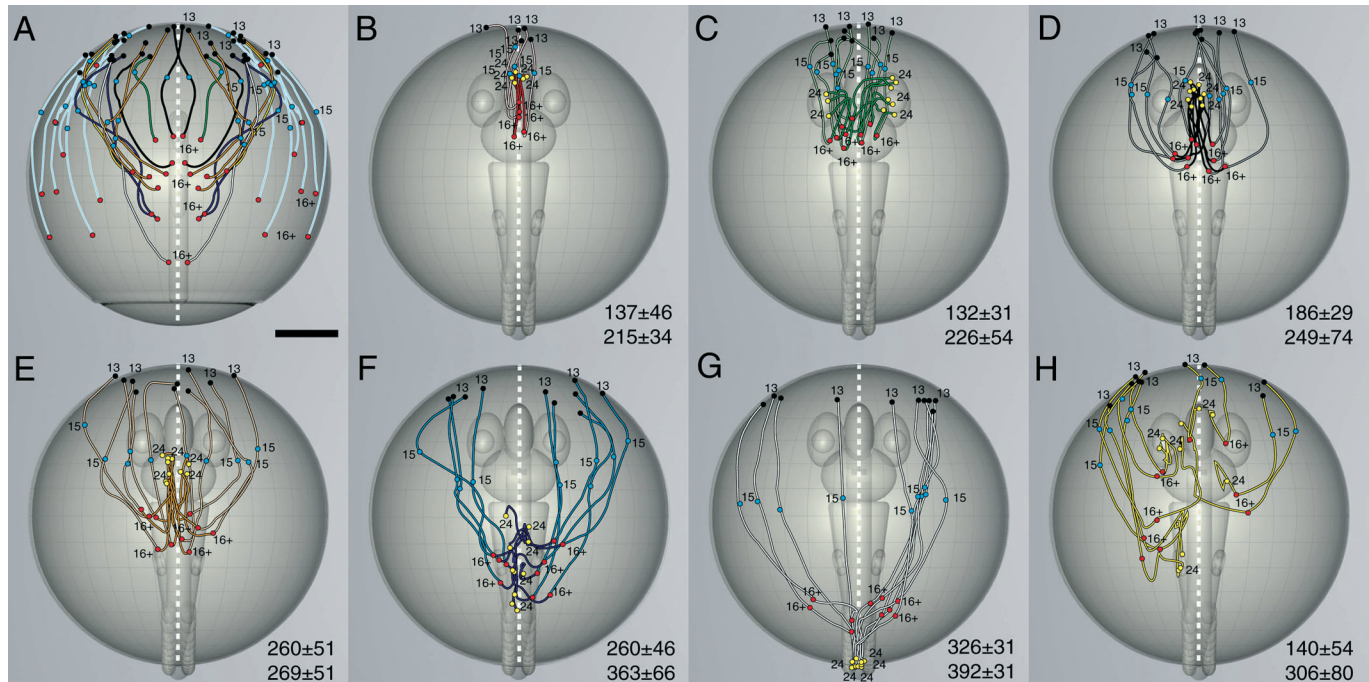
(1) Cells contributing to any neural subdivisions all start convergence to the midline after stage 15, and convergence to the midline is over soon after stage 16+, as indicated by trajectory analysis (Fig. 4).

(2) After stage 16+, intermingling of the cell populations

Organization of the cell groups for future neural subdivisions into 'compartments'

It is remarkable that after stage 16+, cells that later contribute to different neural subdivisions are organized into spatially non-overlapping cell groups, and cells stop crossing the boundary, although cell movement within groups reaches a maximum at stage 17 (Fig. 5B, parts b and c). Analysis of cell movement in the AP direction (Fig. 5B, part b) did not detect other boundaries restricting cell movement. Thus, after stage 16+, cell groups to form the future neural subdivisions acquire the characteristics of 'compartments' first defined in *Drosophila* embryos (Garcia-Bellido et al., 1973). These compartments then develop into individual neural subdivisions.

After the compartment boundaries are formed, mitoses occurring adjacent to the boundary with the neighboring compartment never give rise to daughter cells that contribute

Fig. 4. Trajectories of representative cells contributing to distinct neural subdivisions. (A) Distinct trajectories of cells that contributed to neural and non-neural tissues displayed on an embryo model in dorsal view from stage 13 (black dots) to stage 15 (blue dots), and then to stage 16+ (red dots). Trajectories of the cells are color-coded according to the later contributing neural subdivisions, as in Fig. 3: red, telencephalon; green, retina; orange, mesencephalon; blue, rhombencephalon; white, spinal cord; yellow, placode and neural crest derived tissue; light blue, epidermis. (B-H) Trajectories of ten randomly selected cells (with exception of telencephalon, five) that later contributed to different neural subdivisions: (B) telencephalon; (C) retina; (D) diencephalon; (E) mesencephalon; (F) rhombencephalon; (G) spinal cord; (H) tissue of placode and neural crest origin. Colored dots in black, blue, red and yellow indicate cell positions at stage 13 (25% epiboly), stage 15 (50% epiboly), stage 16+ (90% epiboly) and stage 24, respectively. Figures in the bottom right-hand corner indicate the average distance (μm) of migration among the cell groups from stage 13 to stage 15 (upper) and from stage 15 to stage 16+ (lower). Scale bar: 200 μm.

to another compartment, although mitoses in earlier stages of development often resulted in split fate for daughter cells (Fig. 5C). This clonal separation is another feature of compartments. Clonal separation of cells after establishment of the compartment boundary is also demonstrated for later established subdivisions, e.g. rhombomere boundaries of the chicken (Fraser et al., 1990).

Convergence and extension of the neural primordium in Medaka embryo

In an overall view of the genesis of the CNS primordium, precursors for the future CNS first converge towards the midline, and then the entire CNS undergoes AP elongation ('convergence and extension') (Myers et. al., 2002).

As discussed earlier, convergence of neural precursor cells towards the midline occurs almost synchronously in Medaka embryos, starting at stage 15 and ending at nearly stage 16+, and this movement largely separates cells to be fated to the neural and epidermal lineages (Figs 3, 4). This convergence is not accompanied by a significant AP elongation of the territory occupied by the precursor cells for tel-, di-. mes- and rhombencephalon, and retina.
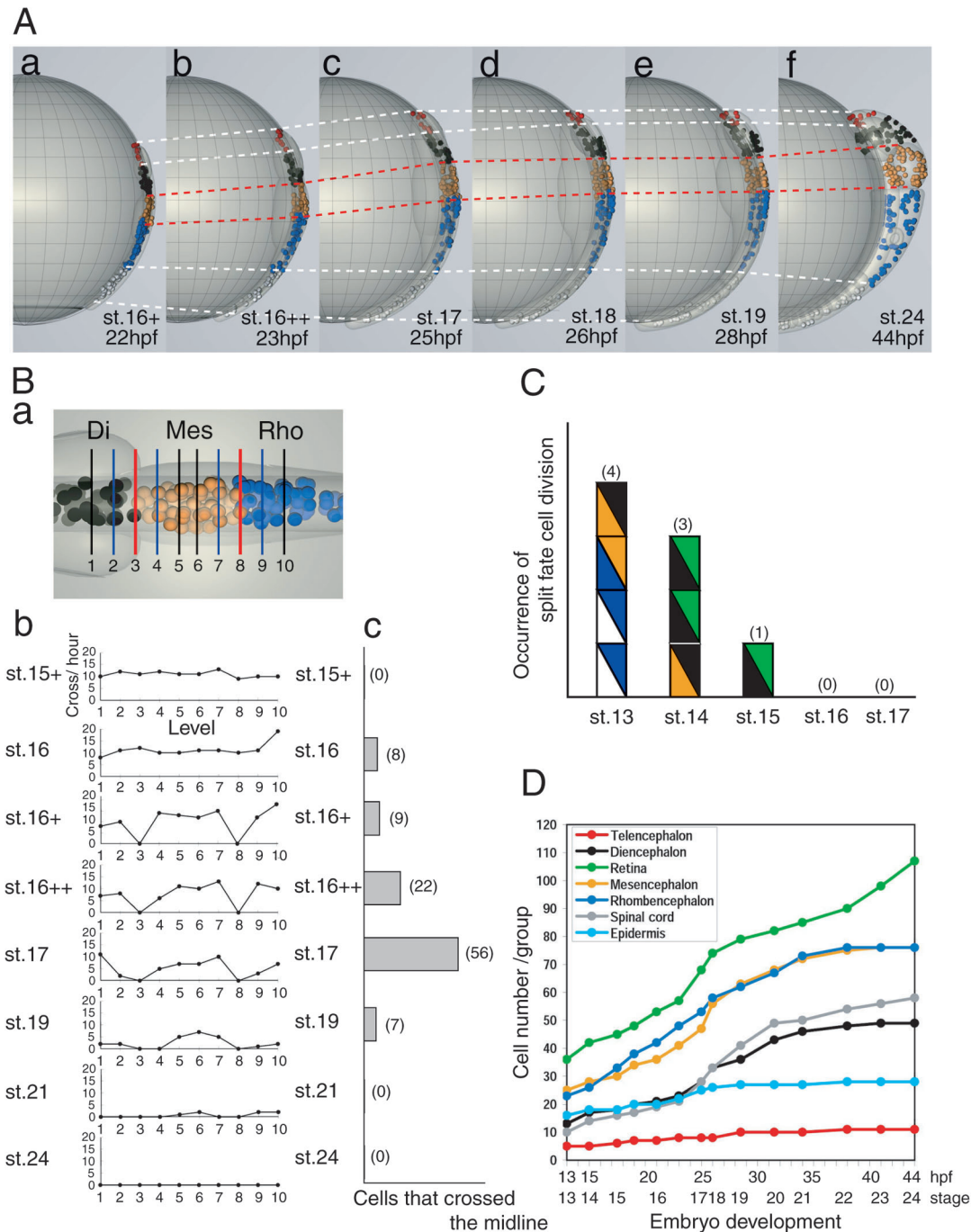
After compartments for neural subdivisions were established at stage 16+ (22 hpf), those for tel-, di- and mesencephalon do not significantly alter their AP length (Fig. 3, Fig. 5A), although the cells increase in individual compartments (Fig. 5A,D). The rhombencephalic subdivision elongates in the AP

dimension two folds by stage 24 (22 hours later), but the gain in tissue thickness was more significant (Fig. 5A). The major part of extension of the CNS primordium is accounted for by elongation of the spinal cord region, which appears to be caused at least in part by cell multiplication (Fig. 5A), and also probably by tissue addition under influence of the 'tail organizer' (Agathon et al., 2003). In the report by Kimmel et al. (Kimmel et al., 1994) on zebrafish embryos where cell clones contributing to the rhombencephalic region were analyzed, extension of the neural tube by an intercalation mechanism was suggested. Analogous mechanisms may also be involved in Medaka development, but this must be only in rhombencephalon and spinal cord regions.
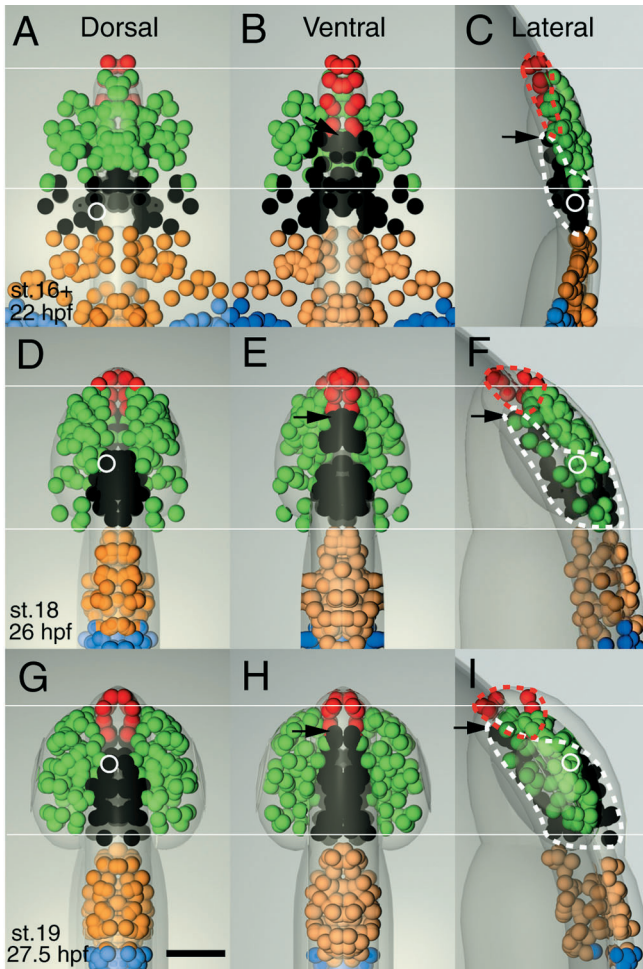
Bifurcation of retinal compartment

An important observation in this study was that retinal precursor cells at first form a single compartment at stage 16+, being separated from the compartments for future telencephalon and diencephalon, and located dorsal to tel- and diencephalic compartments (Figs 3, 6). Then the retinal precursors are split into bilateral retinas, which is associated with dorsal rise and anterior shift of the diencephalic precursors (Fig. 6). This two-step mechanism to produce bilateral retinas was first proposed by cell fate tracing experiments in zebrafish embryos (Varga et al., 1999). When prospective retina and diencephalic cells in the superficial region of zebrafish embryos were labeled at 80% epiboly stage,
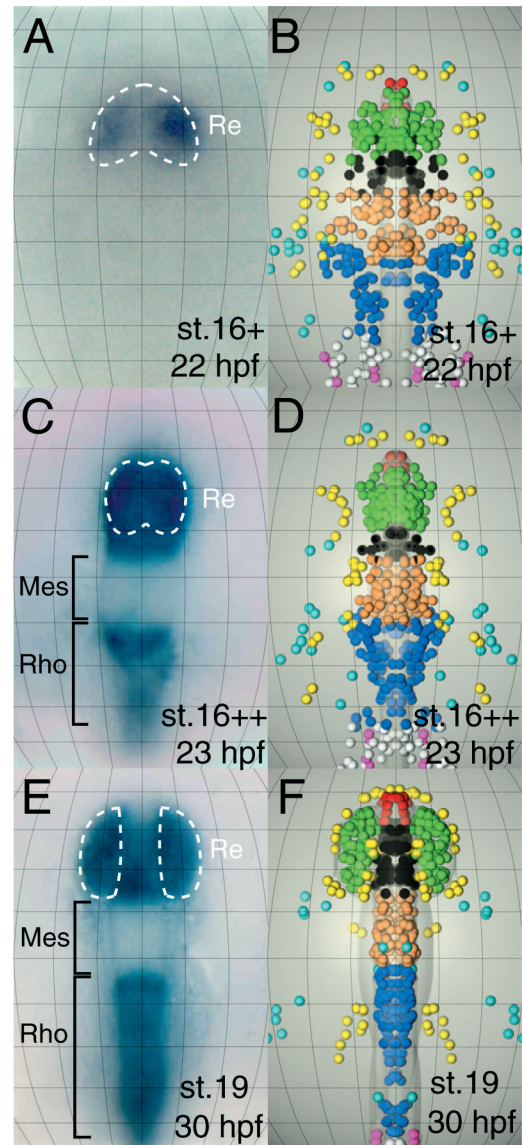
Fig. 5. Establishment of the compartments for future neural subdivisions at stage 16+. (A) Location in embryo and size of the cell groups later contributing to distinct cephalic divisions, color-coded according to Fig. 3. Lateral view of tel-, di-, mes- and rhombencephalon, and spinal cord cell groups from stage 16+ (a) to stage 24 (f). Animal pole on the top and dorsal side on the right. White and red broken lines outline the boundaries for future neural subdivisions. The cell groups for tel-, di- and mesencephalon are displaced anteriorly without changing their AP length, while those for rhombencephalon and spinal cord elongate along the body axis. (B) Measurement of cell movement within cell groups. (a) Horizontal planes across the CNS-forming cell mass to measure cell movement along the AP axis. The planes were drawn on a computer graphics embryo model, so that planes 3 and 8 are placed at the position corresponding to the boundaries at stage 16+ between diencephalon- and mesencephalon-forming cell groups (plane 3) and between mesencephalon- and rhombencephalon-forming cell groups (plane 8). Other planes were drawn at intervals of 40 μm, corresponding to a two-cell width distance. (b) Number of cells crossing the transverse planes (1-10) in an hour was counted at stages indicated. (c) Number of cells crossing the midline at the stage indicated. (C) Occurrence of mitotic cell divisions giving rise to split fate daughter cells. Divisions that produced daughter cells that contributed to different neural subdivisions at stages 13-17 are indicated by two colored rectangles of the color code, as in Fig. 3. Numbers on the top indicate the split cell fate division in each stage. (D) Proliferation of labeled cell populations in cell groups that contributed to particular neural subdivisions at stage 24. Increase in cell number is robust between stage 17 and stage 19, but thereafter becomes moderate except in retina.

Fig. 6. Spatial reorganization of the diencephalic and telencephalic compartments in relation to lateral splitting of retinal compartment. (A,D,G) Dorsal, (B,E,H) ventral and (C,F,I) lateral views of stage 16+, 18 and 19 embryos. (A-C) At stage 16+, retinal precursors form a single compartment overlying telencephalic and diencephalic compartment at their posterior and anterior halves. (D-F) Around stage 18, retinal precursors begin to split bilaterally starting from the posterior side, accompanied by intrusion of the anterior diencephalic compartment. (G-I) By stage 19, lateral splitting of retinal compartment is complete. (C,F,I) Lateral views demonstrating anterodorsal movement of the diencephalic compartment (white broken line) and dorsal movement of the telencephalic compartment (broken red line), relative to the retinal compartment. White lines indicate anterior and posterior limits of the retinal precursors. The white circle follows a single diencephalic precursor cell that moved in an anterior and dorsal direction (A,D,G). (C,F,I) The black arrows follow the anterior movement of a ventrally located diencephalic precursor cell. Scale bar: 100 μm.

Fig. 7. *Pax6* expression and establishment of neural compartments. (A,C,E) *Pax6* expression and (B,D,F) corresponding regions of the computer graphics model. Broken lines surround cells of prospective retina. (A,B) At stage 16+ (22 hpf), *Pax6* expression is first detected in a pair of lateral domains that include future lateral retinal cells, while prospective retinal cells in the middle do not express *Pax6* yet. (C-F) After stage 16++ (23 hpf), *Pax6* is now strongly expressed in the entire prospective retina, diencephalic cells and r1-r2 region of rhombencephalon, and moderately in the remaining part of the prospective rhombencephalon and spinal cord.

and their tissue contribution was analyzed at a later stage (24 hpf), retinal precursor cells clearly formed a single planar cell group distinct from diencephalic precursors. Diencephalic precursors, initially located posterior to the retinal precursors, were later located medial and anterior to the bilateral retinas. In this study using Medaka embryos, we followed the position of individual labeled cells at close intervals, and successfully monitored the cells even those located deep in the embryonic tissue. Thus, spatial reorganization of the compartmentalized

cell groups was clearly displayed in the three dimensional model (Fig. 6). This not only confirms the previous proposal (Varga et al., 1999), but also establishes the two-step retinal splitting mechanism associated with anterior movement of the diencephalic precursors. This mechanism must be common to teleosts, and may presumably be conserved in other vertebrate species.

However, it has been a generally accepted view that prechordal plate mesoderm ventral to the prosencephalons produces signals along the midline that transform retinal

precursors into a non-retinal fate, thus yielding two bilateral retinal cell populations (e.g. Li et al., 1997). This view is based on investigations of early retina development in non-fish vertebrates involving grafting or ablating a cell sheet. In these experiments, cell populations located in the medial part of the retina field appeared bipotential for development into retina and diencephalon (e.g. Couly and Le Douarin, 1988; Fernandez-Garre et al., 2002; Li et al., 1997). Considering the situation in Medaka, the possibility exists that in avian and amphibian species, retinal and diencephalic divisions are also separated earlier than the current model and extensively overlap vertically. This vertical overlap is demarcated in zebrafish by *foxb1.2* (*mar*) gene expression in prospective median hypothalamic precursors (Varga et al., 1999). Thus, the bipotential nature of cell populations observed in grafting experiments could be a consequence of a mixed population of specified retinal and diencephalic cells within grafted pieces of tissues. It is important to re-examine the topology of the primordia of neural divisions in these species, although possible occurrence of species-dependent variation of the mechanism must also be considered.

Another intriguing observation was on the timing of establishment of the retinal compartment and expression of *Pax6* in retinal precursor cells. *Pax6* is known to be involved in establishing characteristics of retina (Grindley et al., 1995) and prosencephalon (Mastick et al., 1997). Shortly after the retinal precursor compartment was established (stage 16+, 22 hpf), expression of *Pax6* was initiated in the lateral retina precursor cells but not in the median retinal precursors (Fig. 7A,B). At stage 16++ (23 hpf, 95% epiboly), *Pax6* expression covered all cells that gave rise to retina, diencephalon and rhombencephalon (Fig. 7C,D). Thus, *Pax6* expression and establishment of the retinal precursor compartment was not synchronous as previously supposed, but initiation of *Pax6* expression in the anterior compartments may depend on cues that were available only to laterally located cells.

It is also interesting to note that in Medaka *eyeless* mutant embryos with low temperature-sensitive *Rx3* expression (Loosli et al., 2001), lateral retinal cells are not formed. However, cells that would normally have the potency to form retina express *Pax6* and have lens-inducing potential. These cells are embedded as a cell cluster in the prospective diencephalic region of the neural plate (Winkler et al., 2000). It is tempting to speculate that the *eyeless* defect lies in the process of bifurcating the retinal cell group at stage 17. Results from a temperature shift experiment (Winkler et al., 2000), where the formation of bilateral retinas is blocked by low temperatures at stage 17, would be consistent with this model.

Thus, analysis of specific gene expression and developmental defects of mutant brains based on the cell tracing technique described here is promising for shedding a new light on principles of early neural development.

References

Agathon, A., Thisse, C. and Thisse, B. (2003). The molecular nature of the zebrafish tail organizer. *Nature* **424**, 448-452.

Ballard, W. (1973). A new fate map for *Salmo gaidneri*. *J. Exp. Zool.* **184**, 49-74.

Couly, G. and Le Douarin, N. M. (1988). The fate map of the cephalic neural primordium at the presomitic to the 3-somite stage in the avian embryo. *Development Suppl.* 101-113.

Fernandez-Garre, P., Rodriguez-Gallardo, L., Gallego-Diaz, V., Alvarez, I. S. and Puelles, L. (2002). Fate map of the chicken neural plate at stage 4. *Development* **129**, 2807-2822.

Fraser, S., Keynes, R. and Lumsden, A. (1990). Segmentation in the chick embryo hindbrain is defined by cell lineage restrictions. *Nature* **344**, 431-435.

Garcia-Bellido, A., Ripoll, P. and Morata, G. (1973). Developmental compartmentalisation of the wing disk of Drosophila. *Nat. New Biol.* **245**, 251-253.

Grindley, J. C., Davidson, D. R. and Hill, R. E. (1995). The role of Pax-6 in eye and nasal development. *Development* **121**, 1433-1442.

Hatada, Y. and Stern, C. D. (1994). A fate map of the epiblast of the early chick embryo. *Development* **120**, 2879-2889.

Inoue, T., Nakamura, S. and Osumi, N. (2000). Fate mapping of the mouse prosencephalic neural plate. *Dev. Biol.* **219**, 373-383.

Ishida, J. (1944). Hatching enzyme in the fresh-water teleost, *Oryzias latipes*. *Annot. Zool. Japon* **22**, 137-154.

Iwamatsu, T. (1994). Stages of normal development in the medaka Oryzias latipes. *Zool. Sci.* **11**, 825-839.

Kimmel, C. B., Warga, R. M. and Schilling, T. F. (1990). Origin and organization of the zebrafish fate map. *Development* **108**, 581-594.

Kimmel, C. B., Warga, R. M. and Kane, D. A. (1994). Cell cycles and clonal strings during formation of the zebrafish central nervous system. *Development* **120**, 265-276.

Kimmel, C. B., Ballard, W. W., Kimmel, S. R., Ullmann, B. and Schilling, T. F. (1995). Stages of embryonic development of the zebrafish. *Dev. Dyn.* **203**, 253-310.

Li, H., Tierney, C., Wen, L., Wu, J. Y. and Rao, Y. (1997). A single morphogenetic field gives rise to two retina primordia under the influence of the prechordal plate. *Development* **124**, 603-615.

Loosli, F., Koster, R. W., Carl, M., Krone, A. and Wittbrodt, J. (1998). Six3, a medaka homologue of the Drosophila homeobox gene sine oculis is expressed in the anterior embryonic shield and the developing eye. *Mech. Dev.* **74**, 159-164.

Loosli, F., Winkler, S., Burgtorf, C., Wurmbach, E., Ansorge, W., Henrich, T., Grabher, C., Arendt, D., Carl, M., Krone, A. et al. (2001). Medaka eyeless is the key factor linking retinal determination and eye growth. *Development* **128**, 4035-4044.

Mastick, G. S., Davis, N. M., Andrew, G. L. and Easter, S. S., Jr (1997). Pax-6 functions in boundary formation and axon guidance in the embryonic mouse forebrain. *Development* **124**, 1985-1997.

Myers, D. C., Sepich, D. S. and Solnica-Krezel, L. (2002). Convergence and extension in vertebrate gastrulae: cell movements according to or in search of identity? *Trends Genet.* **18**, 447-455.

Oppenheimer, J. M. (1936). Processes of localozation in developing fundulus. *J. Exp. Zool.* **73**, 405-444.

Varga, Z. M., Wegner, J. and Westerfield, M. (1999). Anterior movement of ventral diencephalic precursors separates the primordial eye field in the neural plate and requires cyclops. *Development* **126**, 5533-5546.

Wakamatsu, Y., Pristyazhnyuk, S., Kinoshita, M., Tanaka, M. and Ozato, K. (2001). The see-through medaka: a fish model that is transparent throughout life. *Proc. Natl. Acad. Sci. USA* **98**, 10046-10050.

Warga, R. M. and Nusslein-Volhard, C. (1999). Origin and development of the zebrafish endoderm. *Development* **126**, 827-838.

Winkler, S., Loosli, F., Henrich, T., Wakamatsu, Y. and Wittbrodt, J. (2000). The conditional medaka mutation eyeless uncouples patterning and morphogenesis of the eye. *Development* **127**, 1911-1919.

Wittbrodt, J., Shima, A. and Schartl, M. (2002). Medaka – a model organism from the far Eastage. *Nat. Rev. Genet.* **3**, 53-64.

Woo, K. and Fraser, S. E. (1995). Order and coherence in the fate map of the zebrafish nervous system. *Development* **121**, 2595-609.

Woo, K. and Fraser, S. E. (1998). Specification of the hindbrain fate in the zebrafish. *Dev Biol.* **197**, 283-296.